Nonlinear propagation of picosecond pulses interacting with a three-level system

J. Y. Bigot and B. Hönerlage
Laboratoire de Spectroscopie et d'Optique du Corps Solide, Université Louis Pasteur, 5, rue de l'Université, 67084 Strasbourg Cedex, France
(Received 9 May 1986; revised manuscript received 27 January 1987)

We study the evolution in time and in one space coordinate of picosecond laser pulses interacting with a nonlinear medium modeled by three quantum states. This is done by solving numerically the equation of evolution of the density matrix elements together with the Maxwell equation. The nonperturbative treatment of the density matrix allows us to understand the contribution of the different optical transitions and populations to the pulse deformation during its propagation. We apply the model to CuCl where the quantum levels are the fundamental, the excitonic, and the biexcitonic states. Near the two-photon resonance, the pulse is strongly altered and the excitonic and biexcitonic levels show a population inversion. A modulation of the amplitude and a superbroadening of the phase occur during the propagation.

I. INTRODUCTION

When studying the properties of a nonlinear medium, one is confronted with the problem of how the time evolution of the laser excitation influences the nonlinear process which is being analyzed. In the case of a short-pulsed laser source, the polarization of the medium changes the temporal pulse shape which in turn influences the characteristics of the medium, thus leading to a phenomenon of nonlinear propagation.

A successful model to describe this propagation in a one-photon resonant medium is the semiclassical Maxwell-Bloch set of equations. It has led to the understanding of coherent effects such as self-induced transparency[1] which is a solitonlike propagation of the pulse, self-phase modulation[2] which results in a spectral broadening of the laser pulse, self-steepening of the pulse amplitude,[3] and self-focusing or defocusing[4] which are transverse spatial effects. In the case of two-photon resonant media, a similar approach has been chosen by several authors.[5–7] In these works, the medium has been modeled by a three-level system between which optical transitions occur due to the coupling with the electromagnetic field. Using appropriate unitary transformations, the problem has been reduced to the study of a two-level system equivalent to the vector model of Feynman *et al.*[8] With this model and by using the adiabatic following approximation (AFA), Grischkowsky *et al.*[9] have calculated the polarization of the medium and have shown the important contribution of two-photon processes to the nonlinear polarization. However, when the temporal width τ_p of the pulse is such that $\tau_p > \tau_2$, the energy stored in the system through incoherent processes may be very high and the AFA is no longer valid.[10,11] This is, for instance, the case in systems showing a strong absorption or when being excited at resonance. Though an exact solution of the three-level problem was given in Ref. 7 in the case of resonant excitation, to our knowledge no study valid outside and at the resonance was made for excitation pulses longer than the relaxation time τ_2. Since analytic calculations cannot be pursued very far in this temporal range, the solution of the coupled light-matter equations of propagation needs a computational analysis.

The temporal range we investigate is between the coherence relaxation τ_2 and the radiative lifetime τ_1 of the quasiparticles ($\tau_1 > \tau_p > \tau_2$). The pulse width τ_p is then too short for using a stationary analysis but it is too long for assigning pulse deformations to purely coherent effects. From an experimental point of view, this temporal range, which we will call the intermediate region, is often considered when studying the optical properties of semiconductors close to the fundamental gap. The coherence relaxation time is then in the picosecond scale due to the fast transfer of energy between the carriers. The radiative lifetimes of elementary excitations are in the nanosecond scale as measured for excitons and biexcitons in direct gap semiconductors like CuCl.[12] When usual picosecond sources like Nd:YAG lasers ($\tau_p \simeq 20$ ps) are used (where YAG represents yttrium aluminum garnet), the intermediate temporal region is reached. On the contrary, if the nonlinear material is excited with a nanosecond laser source of width τ_p so that $\tau_p \simeq \tau_1$, the sample can be considered to be in a quasistationary regime where the dynamics of the quasiparticles is still important but where an analysis of the sample response can be performed via the study of the transient renormalized dielectric function.[13] We will discuss below why this approach cannot be applied to the intermediate region.

Before describing the three-level system, we must point out that we are going to treat equations of evolution in time and one space coordinate numerically. This restriction is made to avoid excessive computation time. Our purpose here is rather to give some new results concerning the propagation in a two-photon resonant medium than to give an exhaustive study of all coherent effects that may occur in a real experiment. For instance, observation of diffraction, self-focusing, or defocusing cannot be reproduced with our approach. We refer the reader to the in-

teresting work by Mattar *et al.*[14,15] who have studied these transverse effects in the case of a two-level system using nonuniform computational grids in their numerical integration of propagation equations. Concerning transverse effects, we also mention the study of three-level superfluorescence by Mattar and Bowden.[16] In this work, the influence of a high-intensity pump pulse on the temporal shape of the superfluorescent pulse generated by a nonlinear three-level medium is studied. It gives interesting results concerning the pulse-shape control of a beam by another one. Here, we will rather be interested in self-shaping of the pump pulse due to a two-photon resonant nonlinear process. To treat completely this two-photon process, the selection rules are chosen adequately (see Sec. II).

In Sec. II we describe the theoretical background of the model. In Sec. III we discuss the results obtained with CuCl modeled by a three-level system (fundamental, excitonic, biexcitonic levels) when the medium is excited close to the biexciton resonance.

II. MODEL OF THE INTERACTING THREE-LEVEL SYSTEM

The theory of a three-quantum-state system, interacting with a time-dependent electromagnetic field, can be expressed with different formalisms. We use here a semiclassical formalism where the electric field is described classically by Maxwell's equations and the medium by the density matrix[17] in a dipolar interaction with the field. This approach has been used by several authors and is particularly powerful in nonlinear coherent optics. However, we have to recall the physical limits within which it can be applied. In the quantum theory of light,[18] the electric field is described in a basis of coherent states in which the operators, representing the number of photons and the phase of the field, follow the Heisenberg inequalities. Therefore the phase ϕ and amplitude $\mathcal{E}$ of the field cannot be known simultaneously as for a classical electromagnetic wave. In the limit of high numbers of photons, however, the uncertainty about these two quantities is small enough to consider that the electric field $E(\mathbf{r},t)$ is well described at time t and space coordinate $\mathbf{r}$ by the classical expression

$$E(\mathbf{r},t)=\mathcal{E}(\mathbf{r},t)\cos[\omega t-\mathbf{k}\cdot\mathbf{r}+\phi(\mathbf{r},t)] , \tag{1}$$

where ω and $\mathbf{k}$ stand for the pulsation and wave vector in the vacuum of the electric field. Loudon[19] has shown that the limit of high numbers of photons is reached when the amplitude $\mathcal{E}$ satisfies

$$\frac{\epsilon_0 V}{2\hbar\omega}\mathcal{E}^2 \gg 1 , \tag{2}$$

where ϵ_0 is the vacuum dielectric constant and V the elementary volume. In Sec. III, we show that the parameters of CuCl fulfill the inequality (2). As for the dipole approximation, it is valid as long as the electric field is locally uniform over a spatial range covering the electric dipoles, i.e., when the wavelength of the laser excitation is long compared to the distance between the charged particles of the dipoles. For instance, in most of the direct gap semiconductors, excitons have a spatial extension of less than 100 Å [$\sim$10 Å in the case of CuCl (Ref. 20)] and therefore the dipole approximation is completely justified when the semiconductor is excited with visible laser light.

The dipole Hamiltonian of interaction is then

$$H=H_0-\mu E(\mathbf{r},t) , \tag{3}$$

where μ is the dipole operator and H_0 the Hamiltonian of the three-level system in the absence of light. In the matrix notation, they are given by

$$\mu=\begin{pmatrix} 0 & \mu_{12} & \mu_{13} \\ \mu_{21} & 0 & \mu_{23} \\ \mu_{31} & \mu_{32} & 0 \end{pmatrix} , \tag{4}$$

$$H_0=\begin{pmatrix} E_1 & 0 & 0 \\ 0 & E_2 & 0 \\ 0 & 0 & E_3 \end{pmatrix} . \tag{5}$$

E_i is the energy of the level $|i\rangle$. It must be noticed that in CuCl, $\mu_{13}=\mu_{31}=0$ because of the selection rules and that $E_3/2$ is close to E_2. Therefore the two-photon transition between levels $|1\rangle$ and $|3\rangle$ is enhanced due to the presence of the excitonic resonance at energy E_2. The equation of evolution of the density matrix ρ in the Schrödinger representation is given by

$$\frac{\partial\rho_{ij}}{\partial t}=\frac{i}{\hbar}[\rho,H_0-\mu E(\mathbf{r},t)]_{ij}-\left[\frac{\partial\rho_{ij}}{\partial t}\right]_{\text{relax}} . \tag{6}$$

The relaxation terms $(\partial\rho_{ij}/\partial t)_{\text{relax}}$ account for a damping of coherent transitions (terms ρ_{ij} with $i\neq j$) and populations (terms ρ_{ii}). In the case of an exponential damping, it can be linearized to $\Gamma_{ij}\rho_{ij}$ where $1/\Gamma_{ij}$ ($1/\Gamma_{ii}$) is proportional to the transverse (longitudinal) relaxation time of the system. In highly nonlinear pulsed regimes, however, the dissipation of energy or thermalization of quasiparticles is also nonlinear and Γ_{ij} is no more constant. For this reason, we consider here that the damping variables Γ_{ij} depend on the populations ρ_{ii} and ρ_{jj} on levels $|i\rangle$ and $|j\rangle$.

$$\Gamma_{ij}=\Gamma_{ij}^0+a_{ij}^{(i)}\rho_{ii}+a_{ij}^{(j)}\rho_{jj} , \tag{7}$$

where Γ_{ij}^0 is the damping constant in the low-excitation regime and $a_{ij}^{(i)}$ ($a_{ij}^{(j)}$) are the coupling parameters which take into account the collisions on the different levels. We want to stress that the value of these phenomenological parameters can be deduced from experiments but they have not been studied extensively up to now. In Sec. III, we discuss these values in the case of CuCl. Instead of relation (7) another possibility would be to take damping variables proportional to the electric field amplitude $\mathcal{E}$. However, since the damping due to collisions is directly related to the density of quasiparticles and since this density does not follow in time the electric field amplitude (as will be demonstrated by our numerical results in Sec. III), relation (7) is more appropriate for the description of the dynamics. A nonphenomenological study of the population dependence of dampings would require a full treatment of collisions in the nonlinear medium. Several-

particle interactions can be considered by adding an extra term in Eq. (3) which would consist of a screened potential seen by a given particle in the presence of the other particles. Although such processes have been considered[21] in a stationary regime of excitation, their theoretical study under pulsed excitation is not well known up to now. Their consideration is beyond the scope of this paper in which we will discuss only qualitatively the influence of $a_{ij}^{(i)}$ and $a_{ij}^{(j)}$.

To take into account the longitudinal propagation of the amplitude and phase of the pulse, we use the Maxwell equations in the slowly-varying-envelope approximation,

$$\frac{\partial \mathcal{E}(z,t)}{\partial z}+\left[\frac{k}{\omega}+\frac{\epsilon_b}{c^2}\frac{\omega}{k}\right]\frac{\partial \mathcal{E}(z,t)}{\partial t}=\frac{\omega^2}{2k\epsilon_0 c^2}\mathcal{P}_2(z,t)\ ,$$
$$\mathcal{E}(z,t)\frac{\partial \phi(z,t)}{\partial z}+\mathcal{E}(z,t)\left[\frac{k}{\omega}+\frac{\epsilon_b}{c^2}\frac{\omega}{k}\right]\frac{\partial \phi(z,t)}{\partial t}=\frac{\omega^2}{2k\epsilon_0 c^2}\mathcal{P}_1(z,t)\ , \tag{8}$$

where ϵ_b is the background dielectric constant of the medium and $\mathcal{P}_1(z,t),\mathcal{P}_2(z,t)$ are the real and imaginary parts of the polarization $P(z,t)$ which is determined by the density operator $\rho(z,t)$ and the dipole operator μ, according to

$$P(z,t)=\mathcal{P}(z,t)e^{i(\omega t-kz)}\ ,$$
$$\mathrm{Re}P(z,t)=\mathrm{tr}[\rho(z,t)\mu]\ . \tag{9}$$

The set of equations (6)–(9) describes the three-level system in interaction with the classical field $E(z,t)$. Some approximations are usually introduced. The system (6) contains the rotating part $\cos[\omega t-kz+\phi(z,t)]$ of the field. It can be eliminated to avoid unnecessary computation time. Indeed, if we integrated Eq. (8) numerically, we would require a temporal discretization less than the period of the electric field. For a pulse of 10 ps duration at a wavelength of 0.4 μm this would lead to about 10^6 iterations.

We first write (6) in the more convenient form

$$\frac{\partial \rho(z,t)}{\partial t}=[\mathcal{L}_0+\mathcal{L}_1 E(z,t)]\rho(z,t)\ , \tag{10}$$

where $\rho,\mathcal{L}_0,\mathcal{L}_1$ are 3×3 matrices, $\mathcal{L}_0$ and $\mathcal{L}_1$ being time independent and obtained from Eq. (6). We then make the following ansatz:

$$\rho(z,t)=\sum_{n=-\infty}^{+\infty}\rho^n(z,t)e^{in[\omega t+\phi(z,t)]}\ . \tag{11}$$

Then (10) becomes

$$\frac{\partial \rho^n(z,t)}{\partial t}=\left[in\left[\omega+\frac{\partial \phi(z,t)}{\partial t}\right]I_d-\mathcal{L}_0\right]\rho^n(z,t)$$
$$+\mathcal{L}_1\mathcal{E}(z,t)[\rho^{n-1}(z,t)+\rho^{n+1}(z,t)]\ , \tag{12}$$

where I_d is the 3×3 unity matrix. The infinite set of differential equations (12) is now truncated, but all resonant multiple photon transitions are kept. We have shown in a previous publication[22] that in the stationary case ($\partial\rho^n(z,t)/\partial t=0$), all the components of order n with $|n|>2$ have a minor influence on the nonlinear dielectric function (changes of less than $\frac{1}{100}$ of the absorption and dispersion were reported). We will therefore truncate the system at order $|n|=2$. This restriction is not a perturbative theory with respect to the electric field since only the nonresonant n photon transitions are neglected.

Another approximation made by Grischkowski *et al.*[9] is the adiabatic following model. This approximation has the great advantage to lead to an analytical expression for the polarization $P(z,t)$ but it is not appropriate for systems which show a strong absorption or when working in the intermediate temporal region $\tau_1>\tau_p>\tau_2$ defined in the Introduction. For these reasons, we will instead make a numerical analysis of the system (12) simultaneously with Eqs. (8).

We have used a central-difference method of integration for space-dependent variables. For the temporal integration, we used a fifth-order predictor-corrector Adam method. As for the boundary conditions, we have used the following relations (at $z=0$):

$$\mathcal{E}(0,t)=\mathcal{E}_0 e^{-[(t-t_0)/\tau]^2}\ , \tag{13a}$$
$$\phi(0,t)=2\pi\ , \tag{13b}$$
$$\rho_{ij}^n(0,t)=\rho_{ij}^n(0,t_{k-1})\quad \text{for } t_{k-1}\le t<t_k\ . \tag{13c}$$

In (13a) 2τ is the width of the Gaussian pulse. t_0 has been chosen equal to 2τ and the integration is performed between $t=0$ and 4τ. In (13c), t_k is the kth temporal mesh point. The choice of condition (13c) is motivated by the slow decay of the probability transitions ρ_{ij}^n with respect to the temporal mesh size Δt with $\Delta t\ll(\tau_1,\tau_2)$, τ_1,τ_2 being the relaxation times discussed above. We have, however, checked that the solution converges to the same value when taking

$$\rho_{ij}^n(0,t)=0\quad \text{for } (i\neq j \text{ and } i=j\neq 1)\forall n\ , \tag{14a}$$
$$\rho_{11}^0(0,t)=1,\quad \rho_{11}^n(0,t)=0,\quad n\neq 1 \tag{14b}$$

for each step of temporal integration. In this case, however, the computational time is a bit longer. At $z=l$, where l is the sample thickness, the partial differential system is not bound.

As for the initial conditions, we have assumed the following relations for the amplitude of the electric field $\mathcal{E}$ (at $t=0$, $0<z<l$):

$$\mathcal{E}(z,0)=r(\mathcal{E}(0,t))\mathcal{E}_0 e^{-\alpha z-(t_0/\tau)^2}\ . \tag{15}$$

where α is the linear absorption of the field inside the medium and $r(\mathcal{E})$ its reflection coefficient. $r(\mathcal{E})$ is computed at each temporal step t_k with the renormalized quasistationary dielectric function $\epsilon(\omega,t_k)$ according to the model developed in Ref. 13. In the case of CuCl, when we excite a sample close to the two-photon resonance, the reflection $r(\mathcal{E})$ does not change very much the temporal shape of picosecond pulses. This was checked by comparing the results of Sec. III with those obtained with a constant value of the reflection. This is no more the case

when we come very close to the one-photon excitonic resonance where the intensity dependence of the reflection is very important.[23,24]

For the phase ϕ, the probability transitions ρ_{ij}^n, and the populations ρ_{ii}^n, we have (at $t=0$, $\forall z$)

$$\phi(z,0)=2\pi \ , \tag{16a}$$

$$\rho_{ij}^n(z,0)=0 \quad \text{for } (i\neq j \text{ and } i=j\neq 1), \quad \forall n \tag{16b}$$

$$\rho_{11}^0(2,0)=1 \text{ and } \rho_{11}^n(2,0)=0, \quad n\neq 1 \ . \tag{16c}$$

Expression (15) is motivated by the fact that, at very low intensity, the medium is completely linear with an absorption coefficient α known from experiments. This condition is possible since we consider that, at the initial time $t=0$, the laser pulse is mainly outside the sample with only its tail interacting with the medium. We have tried different values for the absorption coefficient α. The system always converges to the same value but it requires more CPU time when we start with a value of α different from the one obtained at low intensity in a stationary regime.

With the initial and boundary conditions given above, we obtain the value of the different variables $(\mathcal{E},\phi,\rho^n)$ at $z=l$ inside the medium. The reflection on the back surface of the sample is not considered here since our purpose is to study the change of a picosecond pulse shape during its way through the sample. We will see in Sec. III that, for CuCl, the profile of intensity in the direction of propagation is steep enough to neglect the influence of the backward wave on the temporal pulse shape if $l\geq 5$ μm. The coupling of forward and backward waves must, however, be accounted for if one is interested in the switching dynamics of thinner samples placed in a Fabry-Perot cavity. Such considerations led Haus *et al.*[25] to good predictive results concerning the switching times in biexcitonic bistability far from the resonance, where the nonlinear absorption is sufficiently small.

III. NUMERICAL RESULTS FOR THE THREE-LEVEL SYSTEM IN CuCl

CuCl is a direct gap semiconductor with T_d point group symmetry (blende structure).[26] It is possible to create excitons and biexcitons by dipole interaction with a laser beam propagating in the transparent region of the crystal.[27] The group symmetries of these excitonic and biexcitonic quantum states and the Γ_5 symmetry of the dipole operator are such that only the transitions from the ground state (unexcited crystal) to the Γ_5 exciton level and from the Γ_5 exciton level to the Γ_1 biexciton level are allowed.[28] The one-step transition from the fundamental to the biexcitonic level is forbidden and therefore biexcitons can only be created by two-photon transitions. The Γ_5 exciton level is split into Γ_{5T} and Γ_{5L} by exchange interaction, but the longitudinal mode Γ_{5L} cannot be excited directly by a transverse electromagnetic field. The crystal is therefore well modeled by the three quantum states: fundamental, excitonic, and biexcitonic. Due to the coupling between the electric field and the excitonic states, the dispersion in wave vector k of laser photons of energy $\hbar\omega_l$ is no longer linear when we approach the excitonic resonance, leading to the well-known polariton dispersion.[29] Up to densities of 10^{13} photons/cm^3, this polariton dispersion is almost intensity independent. When increasing the density of exciting photons, multiple-photon processes become more and more important, leading to a nonlinear dielectric function which shows an anomaly around half the biexciton energy $E_{\rm bi}/2=3.186$ eV. The resulting dispersion is therefore renormalized by the high density of photons and it can be calculated by a nonperturbative model of the dielectric function. This has been performed with different techniques in case of a stationary excitation: Green's functions techniques,[30,31] density matrix formalism,[32] and operator technique in the Heisenberg representation.[33–35] Concerning these different techniques, the density matrix formalism allows us to consider particle lifetimes and therefore the intermediate time range discussed here in an easy way. In addition, the density matrix ρ is analogous to a distribution function which allows us to deduce average values of any operator O [the polarization P in our case, see Eq. (9)] when calculating the trace $\mathrm{tr}(O\rho)$. Therefore, the knowledge of the evolution of the density matrix elements is not an information particular to a given operator but it concerns all expectation values of observable quantities. Although it is well adapted to fit experiments in which a spectral analysis is performed as in hyper-Raman scattering[36] or four-wave mixing,[37] the stationary excitation model was found to be insufficient to explain experiments in which a temporal analysis was performed. For instance, in optical bistability experiments,[38,39] dynamical effects were reported which can alter dramatically the hysteretic response of the device. A memory effect was found which is characterized by a time-dependent nonlinear absorption in the medium which does not follow instantaneously the pulse envelope.[39] The model was then extended to the dynamical regime of excitation and the dielectric function was calculated in the quasistationary approximation.[13] This approximation is valid only for pulse envelopes of temporal width much longer than the relaxation times of the coherence term ρ_{ij} since it assumes that the amplitude of the electromagnetic field varies slowly during the polarization variation of the medium. In CuCl this relaxation is of some picoseconds for excitons and biexcitons at low intensity of excitation.[40] For pulse excitations of some picoseconds, one must therefore abandon the quasistationary approximation. The second important feature in picosecond experiments is the influence of spatial effects. For instance, if one assumes that polaritons travel in the crystal with a constant group velocity $v=10^{-2}c$, c being the light velocity in vacuum, the time required to cross a sample of 30 μm thickness is about 10 ps which is of the order of the temporal pulse width. One cannot therefore assume a mean field inside the sample.

We first give the whole set of partial differential equations and the value of the parameters for CuCl and we then discuss the results.

We use the following definitions:

$$p_{ij}^n=\rho_{ij}^n+(\rho_{ij}^n)^*, \quad q_{ij}^n=-i\,|\rho_{ij}^n-(\rho_{ij}^n)^*| \ ,$$

$$w_{ij}^n=(\rho_{ii}-\rho_{jj})^n+(\rho_{ii}-\rho_{jj})^{n\,*} \ ,$$

$$z_{ij}^n = -i\,|(\rho_{ii}-\rho_{jj})^n - (\rho_{ii}-\rho_{jj})^{n\,*}|\ ,$$

$$\Delta_{ij}^n = \frac{1}{\hbar}(E_j - E_i) - n\left[\omega - \frac{\partial\phi}{\partial t}\right]\ ,$$

$$\Delta_i^n = -n\left[\omega - \frac{\partial\phi}{\partial t}\right]\ ,$$

$i,j = f$, ex, bi

(fundamental, excitonic, and biexcitonic levels),

$$E_1 = 0,\quad E_2 = 3.2025 \text{ eV},\quad E_3 = 6.372 \text{ eV}\ ,$$

$$\mu_{12} = \left|\frac{\epsilon_0\epsilon_b(E_L^2 - E_T^2)}{2E_T}\Omega 1.602\times 10^{-19}\right|^{1/2}$$

excitonic dipole element (mksA unit),

$$\mu_{23} = \sqrt{300}\,\mu_{12}$$

biexcitonic dipole element,

$$E_L = 3.208 \text{ eV},\quad E_T = 3.2025 \text{ eV}$$

longitudinal and transverse excitons,

$$\epsilon_b = 5$$

background dielectric constant,

$$\Omega = 4\times 10^{-28}\ \text{m}^{-3}$$

unit cell volume. The transverse dampings Γ_{ij} $(i\neq j)$ are given by the relation (7) with

$$\hbar\Gamma_{12}^0 = 2\times 10^{-4}\text{ eV},\ a_{12}^{(1)} = a_{13}^{(1)} = 0\ ,$$

$$\hbar\Gamma_{23}^0 = 2\times 10^{-4}\text{ eV},\ a_{12}^{(1)} = a_{23}^{(2)} = a_{23}^{(3)} = a_{13}^{(3)} = 10\text{ eV}\ ,$$

$$\hbar\Gamma_{13}^0 = 4\times 10^{-4}\text{ eV}\ ,$$

δ_p^0 (Kronecker symbol) .

The set of Eqs. (12) is given by

$$\frac{dp_{12}^n}{dt} = -\Gamma_{12}p_{12}^n - \Delta_{12}^n q_{12}^n + \frac{\mu_{12}\mathcal{E}}{2\hbar}(z_{12}^{n-1} + z_{12}^{n+1}) + \frac{\mu_{13}\mathcal{E}}{2\hbar}(q_{13}^{n-1} + q_{13}^{n+1})\ ,$$

$$\frac{dp_{12}^n}{dt} = -\Gamma_{12}q_{12}^n + \Delta_{12}^n p_{12}^n - \frac{\mu_{12}\mathcal{E}}{2\hbar}(w_{12}^{n-1} + w_{12}^{n+1}) - \frac{\mu_{13}\mathcal{E}}{2\hbar}(p_{13}^{n-1} + p_{13}^{n+1})\ ,$$

$$\frac{dp_{13}^n}{dt} = -\Gamma_{13}p_{13}^n - \Delta_{13}^n q_{13}^n + \frac{\mu_{\text{bi}}\mathcal{E}}{2\hbar}(q_{12}^{n-1} + q_{12}^{n+1}) - \frac{\mu_{\text{ex}}\mathcal{E}}{2\hbar}(q_{23}^{n-1} + q_{23}^{n+1})\ ,$$

$$\frac{dq_{13}^n}{dt} = -\Gamma_{13}q_{13}^n + \Delta_{13}^n p_{13}^n - \frac{\mu_{\text{bi}}\mathcal{E}}{2\hbar}(p_{12}^{n-1} + p_{12}^{n+1}) + \frac{\mu_{\text{ex}}\mathcal{E}}{2\hbar}(p_{23}^{n-1} + p_{23}^{n+1})\ ,$$

$$\frac{dp_{13}^n}{dt} = -\Gamma_{23}p_{23}^n - \Delta_{23}^n q_{23}^n + \frac{\mu_{\text{bi}}\mathcal{E}}{2\hbar}(z_{23}^{n-1} + z_{23}^{n+1}) - \frac{\mu_{\text{ex}}\mathcal{E}}{2\hbar}(q_{13}^{n-1} + q_{13}^{n+1})\ ,$$

$$\frac{dq_{23}^n}{dt} = -\Gamma_{23}q_{23}^n + \Delta_{23}^n p_{23}^n - \frac{\mu_{\text{Bi}}\mathcal{E}}{2\hbar}(w_{13}^{n-1} + w_{13}^{n+1}) + \frac{\mu_{\text{ex}}\mathcal{E}}{2\hbar}(p_{13}^{n-1} + p_{13}^{n+1})\ ,$$

$$\frac{dw_{12}^n}{dt} = -\Gamma_{11}(w_{12}^n - w_0\delta_n^0) - \Delta_2^n(z_{12}^n - z_0\delta_n^0) + \frac{\mu_{\text{bi}}\mathcal{E}}{2\hbar}(q_{23}^{n-1} + q_{23}^{n+1} + q_{\bar{2}\bar{3}}^{n+1} + q_{\bar{2}\bar{3}}^{n-1}) - \frac{\mu_{\text{ex}}\mathcal{E}}{\hbar}(q_{12}^{n-1} + q_{12}^{n+1} + q_{\bar{1}\bar{2}}^{n+1} + q_{\bar{1}\bar{2}}^{n-1})\ ,$$

$$\frac{dz_{12}^n}{dt} = -\Gamma_{11}(z_{12}^n - z_0\delta_n^0) + \Delta_2^n(w_{12}^n - w_0\delta_n^0) - \frac{\mu_{\text{bi}}\mathcal{E}}{2\hbar}(p_{23}^{n-1} + p_{23}^{n+1} - p_{\bar{2}\bar{3}}^{n+1} - p_{\bar{2}\bar{3}}^{n-1}) + \frac{\mu_{\text{ex}}\mathcal{E}}{\hbar}(p_{12}^{n-1} + p_{12}^{n+1} - p_{\bar{1}\bar{2}}^{n+1} - p_{\bar{1}\bar{2}}^{n-1})\ ,$$

$$\frac{dw_{23}^n}{dt} = -\Gamma_{22}(w_{23}^n - w_0'\delta_n^0) - \Delta_3^n(z_{23}^n - z_0'\delta_n^0) + \frac{\mu_{\text{ex}}\mathcal{E}}{2\hbar}(q_{12}^{n-1} + q_{12}^{n+1} + q_{\bar{1}\bar{2}}^{n+1} + q_{\bar{1}\bar{2}}^{n-1}) - \frac{\mu_{\text{bi}}\mathcal{E}}{\hbar}(q_{23}^{n-1} + q_{23}^{n+1} + q_{\bar{2}\bar{3}}^{n+1} + q_{\bar{2}\bar{3}}^{n-1})\ ,$$

$$\frac{dz_{23}^n}{dt} = -\Gamma_{22}(z_{23}^n - z_0'\delta_n^0) + \Delta_3^n(w_{23}^n - w_0'\delta_n^0) - \frac{\mu_{\text{ex}}\mathcal{E}}{2\hbar}(p_{12}^{n-1} + p_{12}^{n+1} - p_{\bar{1}\bar{2}}^{n+1} - p_{\bar{1}\bar{2}}^{n-1}) + \frac{\mu_{\text{bi}}\mathcal{E}}{\hbar}(p_{23}^{n-1} + p_{23}^{n+1} - p_{\bar{2}\bar{3}}^{n+1} - p_{\bar{2}\bar{3}}^{n-1})\ . \tag{17}$$

In (17) we have used the conservation property of the diagonal elements of the density matrix: $\sum_{i=1}^3 \rho_{ii} = 1$.

As discussed in Sec. II the system (17) was truncated such that $|n| \leq 2$. It was solved simultaneously with Eqs. (8) and with the initial and boundary conditions [(13)–(16)]. The parameters which were varied are the photon energy $\hbar\omega$ of the exciting laser, the maximum amplitude $\mathcal{E}_0$ of the incident pulse, and the lifetimes $1/\Gamma_{ii}$ of excitons and biexcitons.

In Fig. 1(a) we have represented the evolution of a Gaussian pulse of 20 ps temporal width. The laser photon energy is slightly below the two-photon resonance, at 3.1855 eV. The maximum incident intensity is 20 MW/cm^2.

In the first few micrometers, up to 5 μm, the pulse experiences only a global attenuation. When it propagates deeper in the crystal, its temporal shape is strongly altered and it presents a double structure. When we look at the time evolution of the different density matrix elements ρ_{ij},

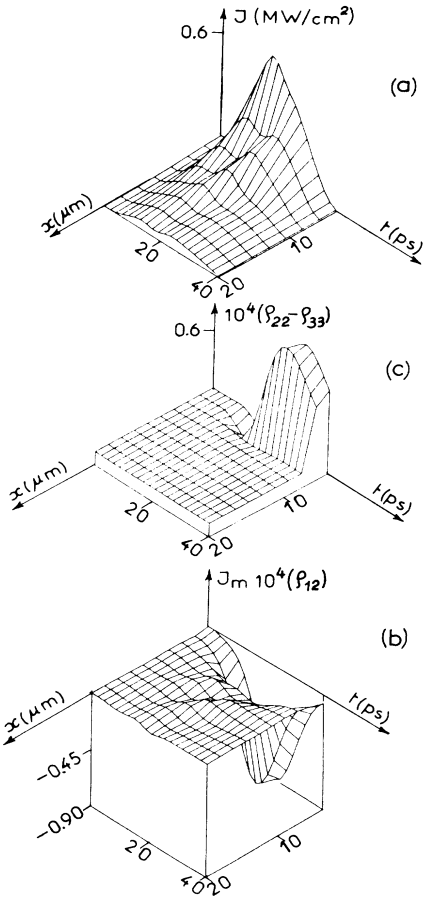

FIG. 1. (a) Propagation of a Gaussian pulse of duration $\Delta t = 20$ ps (FWHM) in a sample of CuCl near the two-photon biexcitonic resonance with a photon energy $\hbar\omega_l = 3.1855$ eV and a maximum incident intensity $I_i^M = 20$ MW/cm^2. (b) Temporal and spatial evolution of the imaginary part of the transition probability ρ_{12} between the fundamental and excitonic levels. (c) Temporal and spatial evolution of the difference of population $(\rho_{22}-\rho_{33})$ between the excitonic and biexcitonic levels.

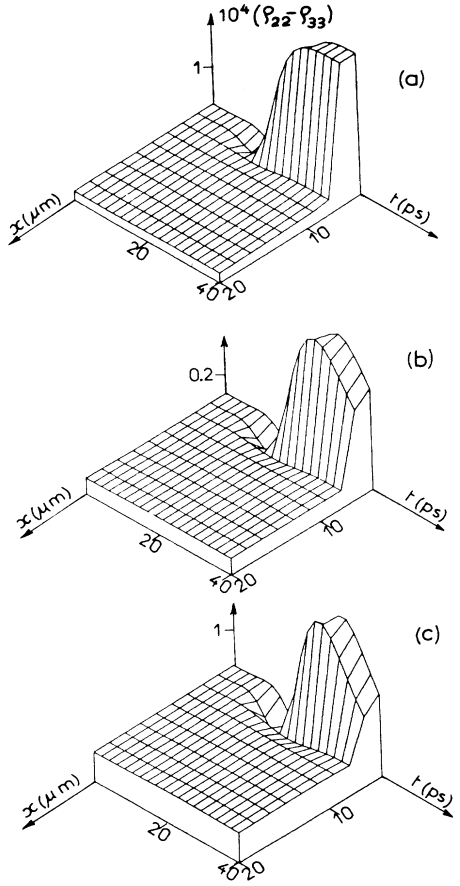

FIG. 2. Temporal and spatial behavior of the difference of population $(\rho_{22}-\rho_{33})$ when exciting a CuCl sample with an incident Gaussian pulse of 40 MW/cm^2 at $\hbar\omega_l = 3.1855$ eV and $\Delta t = 20$ ps, for different lifetimes Γ_{ii} of the levels $|2\rangle$ and $|3\rangle$. (a) $\hbar\Gamma = 10^{-7}$ eV, (b) $\hbar\Gamma = 5\times 10^{-5}$ eV, (c) $\hbar\Gamma = 10^{-4}$ eV.

the same structures appear in $\mathrm{Im}\rho_{12}(t)$ as shown in Fig. 1(b). In the formalism of a time-dependent dielectric function $\epsilon(t)$, the absorption $\alpha(t)$ of the field in the medium is given by[13]

$$\alpha(t) = \frac{\omega_l}{\sqrt{2}c} \left| -\mathrm{Re}\epsilon(t) + \{[\mathrm{Re}\epsilon(t)]^2 + [\mathrm{Im}\epsilon(t)]^2\}^{1/2} \right|^{1/2} \tag{18}$$

and $\mathrm{Im}\epsilon(t)$ is proportional to $\mathrm{Im}\rho_{12}(t)$. Therefore Fig. 1(b) shows that under picosecond excitation, the absorption is not uniform in the bulk of the CuCl sample. In Fig. 1(c) we have plotted the difference of population $(\rho_{22}-\rho_{33})(t)$ between the excitonic and biexcitonic levels. In the very beginning of the sample $(\rho_{22}-\rho_{33})$ is negative, showing that an inversion of population has occurred. This inversion of populations happens later when we are deeper in the crystal. It indicates that the biexciton level plays the role of a reservoir of energy for a certain time. The energy stored in this level is transferred to the excitonic level after a while [$(\rho_{22}-\rho_{33})$ is positive again] and it is then relaxed to the medium. An important feature here is that the time evolution of the difference of populations does not follow the pulse envelope and the relaxation towards equilibrium is achieved after a time which depends on the population lifetimes. This is shown in Fig. 2 where we have varied the longitudinal relaxation constants Γ_{ii}. In Fig. 2(a), for $\hbar\Gamma_{22} = \hbar\Gamma_{33} = 10^{-7}$ eV (long lifetimes) the difference of populations is maximum after the passage of the pulse at 40 ps. When Γ_{ii} is increased [Figs. 2(b) and 2(c)] the equilibrium is found back sooner. The choice of the parameters $a_{ij}^{(k)}$ in Eq. (17) is of minor influence; if their values are increased, the system finds back its steady-state value sooner. The inversion of population shown here when we excite with a 20-ps [full width at half maximum (FWHM)] pulse has also been obtained theoretically with a nanosecond pulsed excitation.[13] We did show that the inversion leads to a saturation of the nonlinear absorption of the medium. An experimental evidence of this behavior has been reported recently.[41] A

temporal analysis of transmission spectra near the two-photon resonance has shown that a gainlike transmission appears at the end of the pulse. It could be related to the dynamics of excitons and biexcitons. According to Fig. 2 we believe that the same behavior should be observed in the picosecond time scale.

The double-structured pulse obtained in Fig. 1(a) has been studied as a function of the maximum intensity I_0 ($I_0 = c\epsilon_0 n \mathcal{E}_0^2/2$). This is shown in Fig. 3 taking the following values: laser photon energy ($\hbar\omega_l = 3.1855$ eV), longitudinal relaxation ($\hbar\Gamma_{22} = \hbar\Gamma_{33} = 10^{-5}$ eV). The spatial variation of the pulses inside the sample is represented from 14 to 20 μm. The same general behavior is obtained in the first few microns. When $I_0 = 1$ MW/cm^2 [Fig. 3(a)] the pulse shape is not altered. For increasing I_0, the pulse deformation develops more and more [Figs. 3(c) and 3(d)].

When we excite with shorter pulses, the number of structures increases. This is shown in Fig. 4(a) for a pulse of 5 ps FWHM. This kind of amplitude modulation due to nonlinear propagation has already been reported earlier in pure coherent systems. One must remember that we are studying here the sample in the intermediate temporal range ($\tau_2 < \tau_p < \tau_1$) where the usual analytical results are not valid. It is of practical interest that similar results are obtained in this region since any nonlinear process as, for instance, wave mixing will probably be very sensitive to this modulation. In Fig. 4(b) we have represented the difference of population ($\rho_{22} - \rho_{33}$) corresponding to the pulse 4(a). One clearly sees the inversion described in Figs. 1 and 2. However, since the pulse is very short, the inversion is maintained until the end of the pulse. Another important feature is that the population distributions do not present the same structured shape as the pulse envelope. Therefore, the structured shapes in Fig. 4(a) (and Fig. 3) cannot be attributed to temporal beatings between

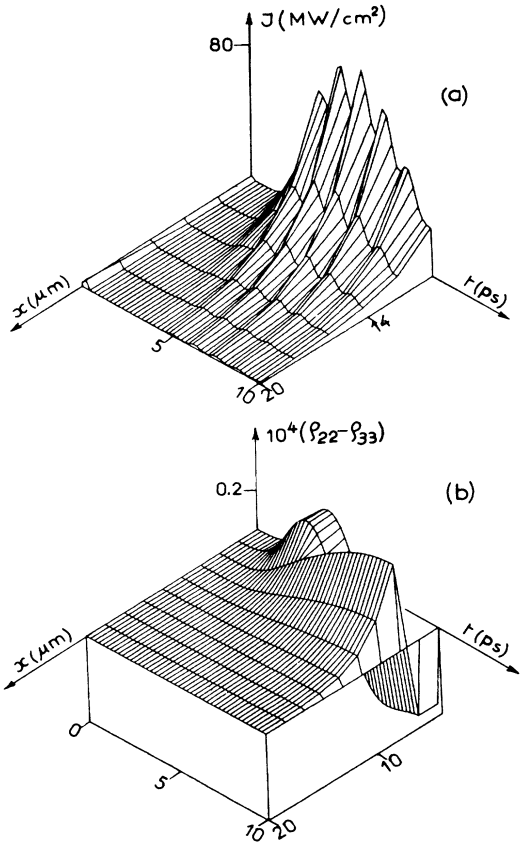

FIG. 4. Propagation of a Gaussian pulse with $\Delta t = 5$ ps showing amplitude modulation (a) and the corresponding behavior of ($\rho_{22} - \rho_{33}$) showing the inversion of population (b). Photon energy of the laser pulse: $\hbar\omega_l = 3.1855$ eV. Maximum incident intensity: $I_i^M = 40$ MW/cm^2.

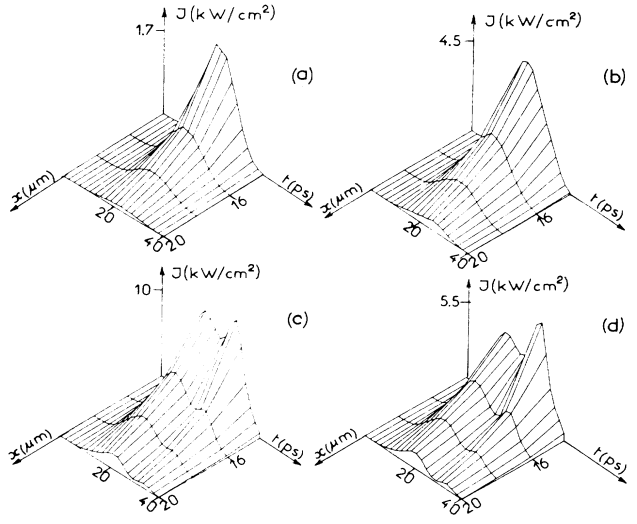

FIG. 3. Propagation of a Gaussian pulse in CuCl with photon energy 3.1855 eV and $\Delta t = 20$ ps, for different maximum incident intensity I_i^M. (a) $I_i^M = 1$ MW/cm^2, (b) $I_i^M = 5$ MW/cm^2, (c) $I_i^M = 20$ MW/cm^2, (d) $I_i^M = 40$ MW/cm^2.

the excitonic and biexcitonic levels.

In Fig. 5 we have varied the photon energy of the incident pulse. The maximum intensity I_0 was fixed to 40 MW/cm^2 and $\hbar\Gamma_{22} = \hbar\Gamma_{33} = 10^{-5}$ eV. Figure 5(a) corresponds to a nonresonant excitation ($\hbar\omega_l = 3.182$ eV). Close to the resonance the temporal structure shows up [5(b), $\hbar\omega_l = 3.1855$ eV]. At resonance [5(c), $\hbar\omega_l = 3.186$ eV], the second structure is slightly less pronounced than in Fig. 3(c). An important result of this work is that a short pulse propagating in the sample of CuCl is not drastically attenuated at the biexciton resonance. This is different when we calculate the absorption α in a quasistationary or stationary regime,[13,22] where a resonant enhancement of absorption was reported. If the transmitted pulses are then calculated within a mean field approximation, the attenuation of the pulse amplitude is overestimated.

We have made our calculations essentially in this spectral region since, as mentioned in Sec. II, our boundary conditions must be revised when we come closer to the one-photon excitonic resonance. Concerning the phase $\phi(z,t)$ of the electric field, its temporal and spatial evolution is given in Fig. 6 for an incident pulse of 10 ps dura-

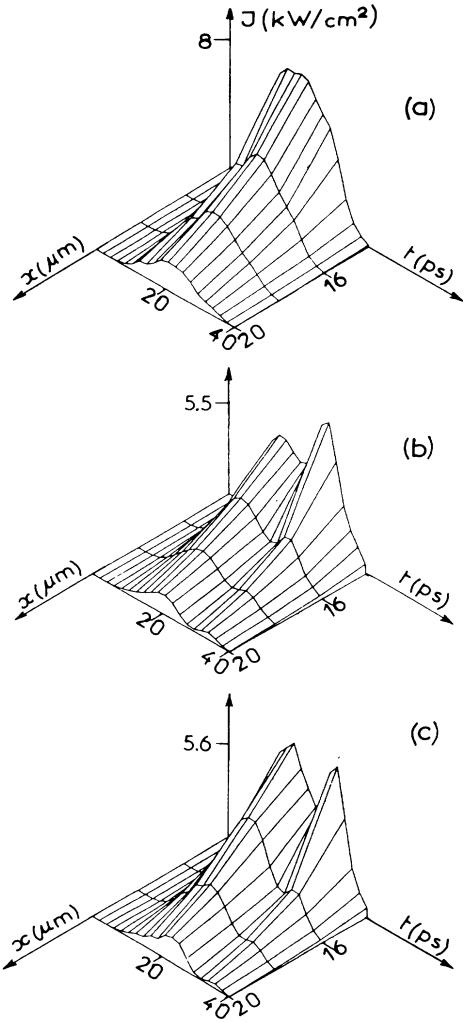

FIG. 5. Propagation of a Gaussian pulse with maximum incident intensity $I_i^M = 40$ MW/cm^2 and $\Delta t = 20$ ps for different photon energies near the biexciton resonance ($E_{bi}/2 = 3.186$ eV). (a) $\hbar\omega_l = 3.182$ eV, (b) $\hbar\omega_l = 3.1855$ eV, (c) $\hbar\omega_l = 3.186$ eV.

tion and maximum intensity $I_0 = 40$ MW/cm^2. The photon energy is 3.1855 eV. Except for the first picoseconds, the phase increases linearly in time. It corresponds to a spectral broadening of the laser pulse which occurs at the very beginning of the pulse after some femtoseconds and which remains constant after 1 ps. This superbroadening increases with I_0, i.e., the slope $\partial\phi(z,t)/\partial t$ is steeper for higher I_0. An experimental analysis of the spectral width of the laser should show such a broadening. A detailed numerical analysis of the phase has still to be made in the case of a femtosecond excitation. Then, as it is well known, the pulse is not monochromatic but at least transformed limited. Although taking into account such a natural linewidth presents no major difficulty, it is beyond the scope of this paper.

Beyond their fundamental interest, the propagation effects reported above have a practical interest since they show that nonlinear devices working in the intermediate

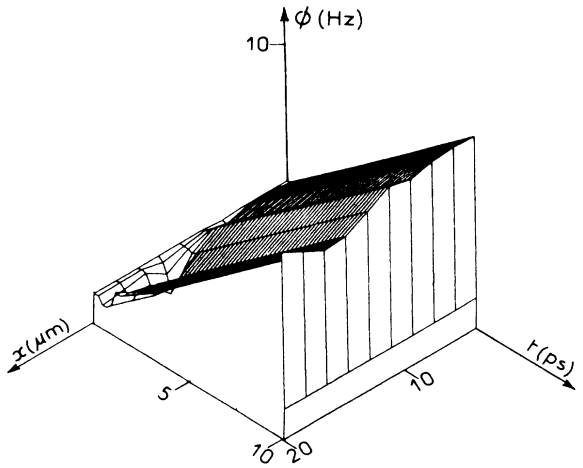

FIG. 6. Temporal and spatial evolution of the phase ϕ of the electric field corresponding to a Gaussian pulse of $\Delta t = 5$ ps duration with a photon energy $\hbar\omega_l = 3.1855$ eV and maximum incident intensity $I_i^M = 40$ MW/cm^2.

temporal region could be affected, for instance, when we try to switch an optical bistable device with a picosecond pulse.

In a two-beam experiment, one should keep in mind that the picosecond pulse is subject to a deformation which is inhomogeneous in space and time. Therefore the switchings of the device can be inhomogeneous too, leading to a complicated transmission of the holding beam.

IV. CONCLUSION

We investigated numerically the interaction of a three-level system with a laser pulse situated in the intermediate temporal region ($\tau_1 > \tau_p > \tau_2$). In the case of CuCl the model shows that the dynamics of excitonic and biexcitonic populations does not follow the pulse envelope and that an inversion between the exciton and biexciton levels shows up. Following previous calculations and experiments in the nanosecond time scale, this inversion should express itself through a gainlike transmission. We have also shown the existence of a superbroadening which should also be seen experimentally. Finally a temporal modulation of the pulse envelope is reported.

ACKNOWLEDGMENTS

The authors are grateful to M. Frindi, J. B. Grun, and R. Levy for many helpful discussions and for a careful reading of the manuscript. They thank M. Simon for his technical assistance. This work was supported by a contract with the "ministère des Postes, Téléphones et Télécommunications (P.T.T.)" of France, Centre National d'Etudes des Télécommunications. It has been carried

out in the framework of an operation launched by the Commission of the European Communities under the experimental phase of the European Community Stimulation Action. The computing facilities used have been attributed by the Conseil Scientifique du Centre de Calcul Vectoriel pour la Recherche. The Laboratoire de Spectroscopie et d'Optique du Corps Solide is "Unité Associée au Centre National de la Recherche Scientifique No. UA232."

[1]S. L. McCall and E. L. Hahn, Phys. Rev. **183**, 457 (1969).
[2]R. G. Brewer, Phys. Rev. Lett. **19**, 8 (1967); F. Shimizu, Phys. Rev. Lett. **19**, 1097 (1967).
[3]D. Grischkowsky, E. Courtens, and J. A. Armstrong, Phys. Rev. Lett. **31**, 422 (1973).
[4]D. Grischkowsky, Phys. Rev. Lett. **24**, 866 (1970); Phys. Rev. A **6**, 1566 (1972).
[5]E. M. Belenov and I. A. Polnekov, Zh. Eksp. Teor. Fiz. **56**, 1407 (1969).
[6]M. Takatsuji, Phys. Rev. A **4**, 808 (1971).
[7]R. G. Brewer and E. L. Hahn, Phys. Rev. A **11**, 1641 (1975).
[8]R. P. Feynman, F. L. Vernon, and R. W. Hellwarth, J. Appl. Phys. **28**, 49 (1957).
[9]D. Grischkowsky, M. M. T. Loy, and P. F. Liao, Phys. Rev. A **12**, 2514 (1975).
[10]D. Grischkowsky, in *Laser Applications to Optics and Spectroscopy,* edited by S. F. Jacobs, M. Sargent III, J. F. Scott, and M. O. Suilly (Addison-Wesley, Reading, Mass., 1975).
[11]E. Courtens, in *Laser Handbook,* edited by F. T. Arecchi and E. O. Schulz-Dubois (North Holland, Amsterdam, 1972), Vol. 2.
[12]R. Levy, B. Hönerlage, and J. B. Grun, Phys. Rev. B **19**, 2326 (1979).
[13]J. Y. Bigot, J. Miletic, and B. Hönerlage, Phys. Rev. B **32**, 6478 (1985).
[14]F. P. Mattar, in *Optical Bistability,* edited by C. M. Bowden, M. Ciftan, and H. R. Robl (Plenum, New York, 1981).
[15]F. P. Mattar and M. C. Newstein, Comput. Phys. Commun. **20**, 139 (1980).
[16]F. P. Mattar and C. M. Bowden, Phys. Rev. A **27**, 345 (1983).
[17]C. Cohen-Tanoudji, B. Diu, and F. Laloë, in *Quantum Mechanics* (Wiley, New York, 1977), Vol. II.
[18]R. J. Glauber, Phys. Rev. **131**, 2766 (1963).
[19]R. Loudon, in *The Quantum Theory of Light* (Oxford University Press, New York, 1977).
[20]R. Levy and J. B. Grun, Phys. Status Solidi A **22**, 11 (1974).
[21]H. Haug and S. Schmitt-Rink, Prog. Quantum Electron. **9**, 3 (1984).
[22]B. Hönerlage and J. Y. Bigot, Phys. Status Solidi B **124**, 221 (1984).
[23]M. Frindi, F. Tomasini, B. Hönerlage, R. Levy, and J. B. Grun, J. Phys. (Paris) Colloque. **46**, C7-215 (1985).
[24]R. Levy, F. Tomasini, J. Y. Bigot, and J. B. Grun, J. Lumin. **35**, 79 (1986).
[25]J. W. Haus, C. M. Bowden, and C. C. Sung, Phys. Rev. A **31**, 1936 (1985).
[26]A. Goltzené and C. Schwab, Prog. Cryst. Growth Character **5**, 233 (1982).
[27]S. Nikitine, A. Mysyrowicz, and J. B. Grun, Helv. Phys. Acta **41**, 1058 (1968); A. Mysyrowicz, J. B. Grun, R. Levy, A. Bivas, and S. Nikitine, Phys. Lett. **26A**, 615 (1968).
[28]J. B. Grun, B. Hönerlage, and R. Levy in *Excitons,* edited by V. M. Agranovitch and A. A. Maradudin (North-Holland, Amsterdam, 1982), Vol. 2.
[29]B. Hönerlage, R. Levy, J. B. Grun, C. Klingshirn, and K. Bohnert, Phys. Rep. **124**, 163 (1985).
[30]R. März, S. Schmitt-Rink, and H. Haug, Z. Phys. B **40**, 9 (1980); H. Haug in *Festkörperprobleme XXII,* edited by J. Treusch (Vieweg Verlag, Braunschweig, 1982), p. 149.
[31]V. May, K. Henneberger, and F. Henneberger, Phys. Status Solidi B **94**, 611 (1979).
[32]J. Y. Bigot and B. Hönerlage, Phys. Status Solidi B **121**, 649 (1984); B. Hönerlage and J. Y. Bigot, Phys. Status Solidi B **123**, 201 (1984).
[33]I. Abram and A. Maruani, Phys. Rev. B **26**, 4759 (1982).
[34]C. C. Sung and C. M. Bowden, J. Opt. Soc. Am. B **1**, 395 (1984).
[35]C. C. Sung, C. M. Bowden, J. W. Haus, and W. K. Chiu, Phys. Rev. A **30**, 1873 (1984).
[36]J. B. Grun, B. Hönerlage, and R. Levy, Solid State Commun. **46**, 51 (1983).
[37]B. Hönerlage, J. Y. Bigot, R. Levy, F. Tomasini, and J. B. Grun, Solid State Commun. **48**, 803 (1983); F. Tomasini, J. Y. Bigot, and R. Levy, J. Phys. (Paris) Colloq. **44**, C5-79 (1983).
[38]R. Levy, J. Y. Bigot, B. Hönerlage, F. Tomasini, and J. B. Grun, Solid State Commun. **48**, 705 (1983).
[39]J. Y. Bigot, F. Fidorra, C. Klingshirn, and J. B. Grun, IEEE J. Quantum Electron. **QE-21**, 1480 (1985).
[40]Vu Duy Phach, A. Bivas, B. Hönerlage, and J. B. Grun, Phys. Status Solidi B **84**, 731 (1977); Vu Duy Phach, A. Bivas, B. Hönerlage, and J. B. Grun, Phys. Status Solidi B **86**, 159 (1978).
[41]J. Y. Bigot, M. Frindi, F. Fidorra, R. Levy, and B. Hönerlage, Phys. Status Solidi B **138**, 622 (1986).
[42]S. A. Akhmanov, R. V. Khokhlov, and A. P. Sukhorukov, in *Laser Handbook,* edited by F. T. Arecchi and E. O. Schulz-Dubois (North Holland, Amsterdam, 1972), Vol. 2.